Autonomous Data-driven Model for Extraction of VCSEL Circuit-level Parameters

Autonomous Data-driven Model for Extraction of VCSEL Circuit-level Parameters

Ihtesham Khan
Politecnico di Torino, IT
ihtesham.khan@polito.it

Lorenzo Tunesi
Politecnico di Torino, IT
lorenzo.tunesi@polito.com

Muhammad Umar Masood
Politecnico di Torino, IT
muhammad.masood@polito.it

Enrico Ghillino
Synopsys, USA
enrico.ghillino@synopsys.com

Vittorio Curri
Politecnico di Torino, IT
curri@polito.it

Andrea Carena
Politecnico di Torino, IT
andrea.carena@polito.it

Paolo Bardella
Politecnico di Torino, IT
paolo.bardella@polito.it

***Abstract*—In recent years, a number of computationally efficient models have been developed that adequately describe the static and dynamic behavior of the Vertical Cavity Surface Emitting Laser (VCSEL). In order to correctly recreate the behavior of existing laser sources, a large number of physical parameters must be specified. Finding these unknown physical characteristics in experimental curves may be time-consuming, and mainly requires trial and error processes or regression analysis. Instead of manually analyzing experimental data to find the best VCSEL parameters, we propose a Machine Learning (ML) based solution to automate the process. The proposed approach exploits the parametric dataset obtained from Light-current and Small-signal modulation responses to extract the required model parameters. Excellent results are obtained in terms of relative prediction error.**

***Index Terms*—Vertical Cavity Surface Emitting Laser, Machine learning, Circuit-level models**

I. Introduction

Lasers are currently utilized in various applications, including data transmission, marking, cutting, additive manufacturing, etc. [1], [2], [3], [4], [5], [6]. In order to provide an insight on the behaviour of these sources and to help in the design process, a large number of models have been developed in the last decades to describe the various families of devices used for those application, each describing the specific properties of the various laser sources and applications.

Approaches based on numerical models provide comprehensive, general solutions via approximation and can include a large number of linear and non-linear physical effects to improve the accuracy of the results. In general, however, it is computationally costly to identify the value of the correct parameters to reproduce the experimental evidence. A comprehensive systematic analysis of all potential combinations of the parametric space is required to identify the ideal parametric blend. This procedure is time-consuming, lasting in some cases days or weeks, and unfocused, squandering energy, time, and money. Simultaneously, once this time-consuming approach identifies the ideal parametric combination, tiny adjustments can alter the optimal operating point, necessitating a fresh round of experimental trials to identify a new optimal combination of parameters. This makes laser modeling extremely difficult for precise and realistic characterization. In this regard, ML has lately proven to be a viable alternative [7], as it can define a model directly from experimental data. The ML-based models are completely agnostic and simply require a substantial size of data to characterize the lasers of various families, which are used in a wide variety of applications.

Various laser families have been introduced during the past few decades, including VCSELs. Recently, numerous computationally efficient models have been developed to precisely define the static and dynamic behavior of VCSELs. These models serve a crucial role in comprehending the physical properties of VCSELs, which enables further optimization of these devices. In addition, they are an essential resource for simulating VCSEL sources as part of larger optoelectronic systems in a realistic manner. In fact, so-called "circuit-level models" of VCSEL are accessible in modeling environments such as the Synopsys OptSim circuit simulation environment [8].

In order to acquire accurate results from the numerical simulation of the entire photonic system, various physical parameters must be specified appropriately in these models to mimic the behavior of current laser sources accurately. We offer a machine learning-based method already applied to laser parametric extraction and inverse design challenges [7]. The suggested ML-based approach to the issue permits the efficient extraction of the necessary VCSEL parameters from experimental data and has the capability to define the parameters in real-time. The suggested solution can be implemented in two phases. The first phase is related to the parameter at a constant temperature, whereas the second phase is related to varying temperatures. Here, the scope of this analysis is to consider the first phase only, i.e., parameters extraction at a constant temperature. Still, the procedure can be easily extended to the second phase also, and it can be applied to different laser families.

The manuscript is organized as follows. In Section II, we describe the main equations of the considered VCSEL model, available in Synopsys OptSim [8]. In Section III, we discuss the generation of the dataset for the ML agent training and validation along with the architecture of the ML model. In

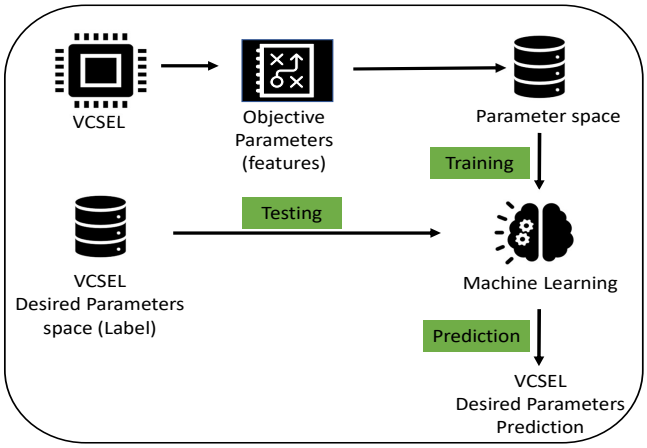

Fig. 1: ML assisted VCSEL parameters extraction.

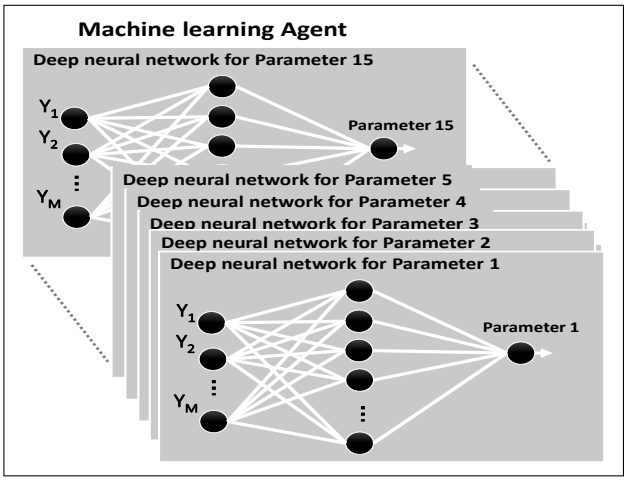

Fig. 2: Parallel architecture of a deep neural network

Section IV, we present the results of such training. Finally, we draw our conclusions in Section V.

TABLE I: Parameters investigated and variation ranges for generating dataset at 25 °C.

Parameter	Range
Current injection efficiency η_i	0.7 to 1
Output power conversion factor k_f	$1{\times}10^8$ to $6{\times}10^8$
Photons lifetime τ_p	2 ps to 3.5 ps
Carrier lifetime τ_n	0.5 ns to 5 ns
Gain coefficient g_0	$-30\,000\,\mathrm{s}^{-1}$ to $-1000\,\mathrm{s}^{-1}$
Gain coefficient parameter $a_{\mathrm{g}0}$	5000 to 30 000
Gain coefficient parameter $b_{\mathrm{g}0}$	1000 to 20 000
Carrier transparency number n_tr	$2{\times}10^6$ to $3{\times}10^7$
Transparency number parameter $c_{\mathrm{n}0}$	−10 to 10
Gain saturation factor ε	$1{\times}10^{-8}$ to $2{\times}10^{-6}$
Leakage current factor I_lo	0 A to $3{\times}10^4$ A
Leakage current empirical parameter a_0	1000 K to 8000 K
Overlap coefficient ρ	0.1 to 1
Diffusion parameter h_diff	1 to 20
VCSEL thermal impedance R_th	$500\,\mathrm{K\,W^{-1}}$ to $8000\,\mathrm{K\,W^{-1}}$

II. Vertical Cavity Surface Emitting Lasers Model

The VCSEL model used for our analysis is an evolution of the model originally proposed in [9]. The current model, implemented in an OptSim block, uses a mean field approach and is based on a set of rate equations.

In cylindrical geometry, the carrier number in the active medium is expanded in the Bessel series, with the position independent terms N_0 and N_1 being considered [9]:

$$N(r) = N_0 - N_1 J_0(\sigma_1 r/R) \tag{1}$$

with σ_1 first non zero root of J_1, r distance with respect to the VCSEL symmetry axis, R active layer radius, $J_0(x)$ and $J_1(x)$ first kind Bessel functions. The rate equations describing the temporal evolution of the spatially independent carrier numbers N_0 and N_1 read

$$\frac{\partial N_0}{\partial t} = \frac{\eta_\mathrm{i} I}{q} - \frac{N_0}{\tau_\mathrm{n}} - \frac{G\left[\gamma_{00}(N_0 - N_\mathrm{t}) - \gamma_{01} N_1\right]}{1+\varepsilon S} S - \frac{I_\mathrm{l}}{q} \tag{2}$$

$$\frac{\partial N_1}{\partial t} = -\frac{N_1}{\tau_\mathrm{n}}(1+h_\mathrm{diff}) + \frac{G\left[\phi_{100}(N_0 - N_\mathrm{t}) - \phi_{101} N_1\right]}{1+\varepsilon S} S \tag{3}$$

with η_i current injection efficiency, I injected current, q electron charge, τ_n carrier lifetime, G gain, γ_{100}, γ_{101}, ϕ_{100} and ϕ_{101} mode overlap coefficients [9] calculated by OptSim as a function of the ratio ρ between the characteristic radius R_m and R, N_t carrier transparency number, ε gain saturation factor, I_l leakage current, and h_diff diffusion parameter.

While parasitic electrical effects can be introduced in OptSim and more realistic bias-tee connections can be included, for the purpose of this study we assume a simple direct drive of the laser. The temporal evolution the photon number in the cavity S is described as

$$\frac{\partial S}{\partial t} = -\frac{S}{\tau_\mathrm{p}} + \frac{\beta_\mathrm{sp} N_0}{\tau_\mathrm{n}} + \frac{G\left[\gamma_{00}(N_0 - N_\mathrm{t}) - \gamma_{01} N_1\right]}{1+\varepsilon S} S \tag{4}$$

with τ_p photons lifetime and β_sp spontaneous emission coefficient. The output power P_out is simply calculated as the product between the cavity photon number and a scaling coefficient k_f.

An additional equation improves the model in [9] allowing to include in the simulation the evolution of the field phase ϕ [10]:

$$\frac{\partial \phi}{\partial t} = \frac{\alpha}{2} \frac{G\left[\gamma_{00}(N_0 - N_\mathrm{tr}) - \gamma_{01} N_1\right]}{1+\varepsilon S} \tag{5}$$

with α linewidth enhancement factor. In order to introduce in the model the effects related to the temperature T, a phenomenological representation of the gain G, the carrier transparency number N_t, an the leakage current I_l is used:

$$G(T) = G_0 \frac{a_{\mathrm{g}0} + a_{\mathrm{g}1} T + a_{\mathrm{g}2} T^2}{b_{\mathrm{g}0} + b_{\mathrm{g}1} T + b_{\mathrm{g}2} T^2} \tag{6}$$

$$N_\mathrm{t}(T) = N_\mathrm{tr}\left(c_{\mathrm{n}0} + c_{\mathrm{n}1} T + c_{\mathrm{n}2} T^2\right) \tag{7}$$

$$I_\mathrm{l}(T) = I_{\mathrm{l}0} \exp\left(\frac{-a_0 + a_1 N_0 + a_2 N_0 T - a_3/N_0}{T}\right) \tag{8}$$

with $I_{\mathrm{l}0}$ leakage factor; a_{g0}-a_{g2}, $b_{\mathrm{g}0}$-$b_{\mathrm{g}2}$, $c_{\mathrm{n}0}$-$c_{\mathrm{n}2}$, and a_0-a_3 are fitting coefficients.

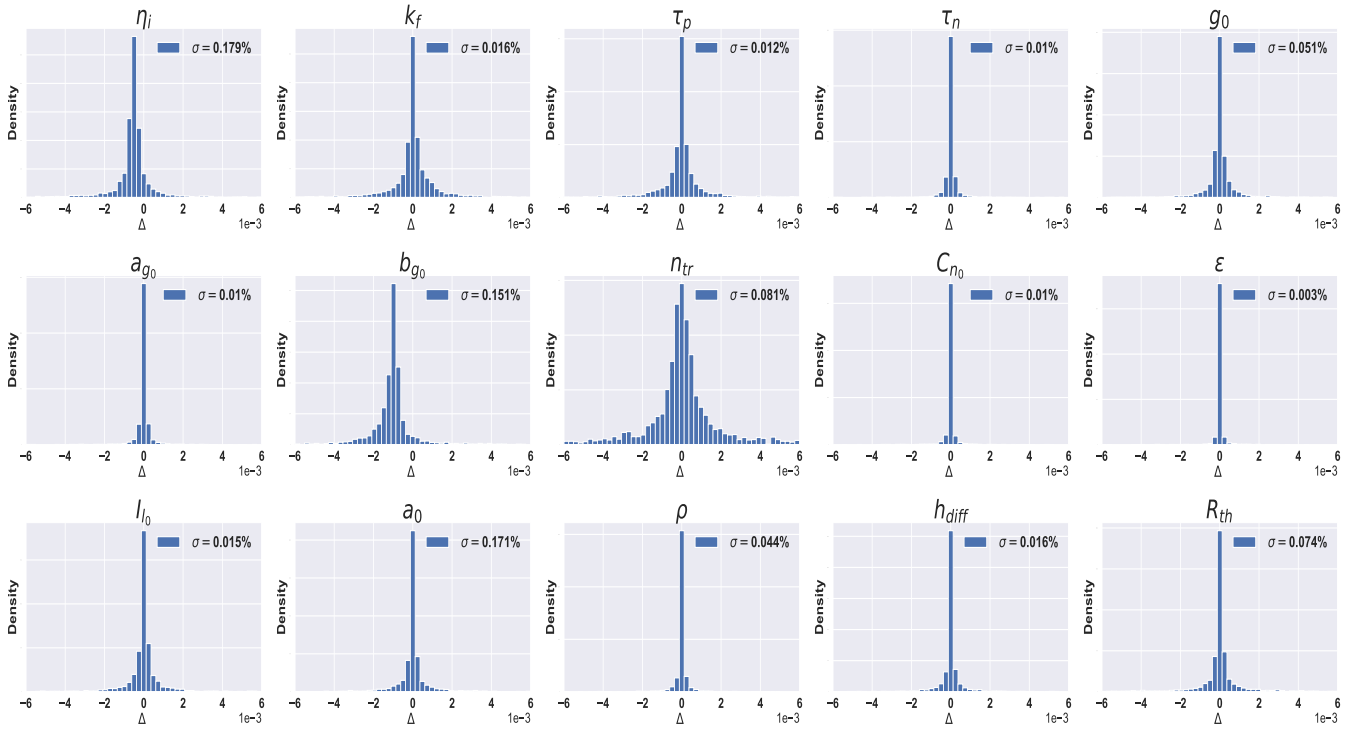

Fig. 3: Relative predicting error of ML agent for the 15 considered parameters. Values in the plot each histogram indicate the relative error standard deviation.

TABLE II: Parameters used to describe the temperature dependence of gain, transparency carrier and leakage current ([9], device B).

Parameter	Value
Gain coefficient parameter a_{g1}	8.282 K^{-1}
Gain coefficient parameter a_{g2}	0.088 46 K^{-2}
Gain coefficient parameter b_{g1}	–49.41 K^{-1}
Gain coefficient parameter b_{g2}	8.2 K^{-2}
Transparency number parameter c_{n0}	6.521
Transparency number parameter c_{n1}	–0.0336 K^{-1}
Transparency number parameter c_{n2}	6.012×10^{5} K^{-2}
Leakage current parameter a_1	1.98×10^{-4} K
Leakage current parameter a_2	9.377×10^{-9}
Leakage current parameter a_3	6.634×10^{8} K

Finally, the device internal temperature is calculated as

$$T = T_{\text{ref}} + (P_{\text{in}} - P_{\text{out}})R_{\text{th}} - \tau_{th}\frac{dT}{dt} \tag{9}$$

with T_{ref} ambient temperature (set to 25 °C for this analysis), P_{in} electrical power entering the device, R_{th} thermal resistance, and τ_{th} thermal time constant.

III. Dataset Generation and Machine Learning Model

We consider a single mode VCSEL emitting at 683 nm. At a constant temperature of 25 °C, the dataset of 10 000 simulations is created by altering the values of the parameters listed in Tab. I and holding the other parameters constant; for the parameters listed in Tab. II the reported value is used, while the remaining parameters are configured with the default values supplied by OptSim. The dataset is populated with 16 samples of the computed Light-current (L-I) curve, generated for linearly spaced injected currents I ranging from 1 mA to 25 mA, an interval consistent with the investigated parameter ranges, for each set of parameters. In addition, small-signal modulation responses are numerically computed [11] at 6 mA, 12 mA, 18 mA, and 24 mA; for each curve, 16 samples are saved at frequencies logarithmically spaced between 10 kHz and 50 GHz. Each dataset record is then composed by $16+16\times 4 = 80$ values.

This work focuses mainly on extracting the 15 parameters provided in Tab. I. The extraction of 15 parameters using a data-driven approach is accomplished by simulating an ML agent primarily based on a Deep neural network (DNN) architecture with three hidden layers and 20 neurons per layer [12]. Mean square error (MSE) is utilized as the loss function in the proposed DNN model. The activation function is *ReLU*. The DNN model is configured with 1000 training steps and a learning rate of 0.01 by default. The training set proportion is 70%, and the test set proportion is 30% of the entire dataset. The suggested DNN is developed utilizing a Deep learning system Toolbox™ of Matlab® platform.

To increase the accuracy of predictions, we suggest a parallel DNN architecture. The DNN agent is trained using a piece of data created at a constant temperature (see Tab. I), and the remaining portion of the same dataset is used to assess

the ML's ability to extract these experimental data parameters as described in Tab. I.

IV. Results and Discussion

In order to assess the DNN unit's accuracy in predicting, we look at the relative prediction error (Δ) for each parameter in the test set:

$$\Delta = \frac{\text{Predicted Value} - \text{Actual Value}}{\text{Actual Value}} \tag{10}$$

In Fig. 3 the ML agent results are shown in a histogram of the relative error of the parameters under consideration, together with the standard deviation (σ) of the relative error histogram. In addition, the MSE for all considered parameters at the completion of the training phase is less than 0.1.

The suggested approach can rapidly obtain an accurate set of VCSEL parameters using a fully automated and agnostic procedure. The simulation requires a few hours of compute time on the most up-to-date workstations to produce the datasets and train the ML agents. Moreover, in a more complex application, the proposed model can be easily scaled up with a high level of accuracy for a larger number of parameters (compared to the 15 parameters analyzed in this work) due to its parallel architecture, which has the capacity to be rapidly expanded without compromising accuracy, enabling the proposed architecture to be advantageously adapted for studying other laser classes.

Finally, for a specific device, temperature related fitting coefficient, listed in Tab. II, can be extracted training an additional network with simulations performed at different temperature. In this condition, parameters listed in Tab. I would be fixed to the value extracted by the first agent and the values in Tab. II would be the returned by the newly trained agent.

V. Conclusions

We proposed an approach based on machine learning that can efficiently extract the necessary VCSEL parameters from experimental data. The proposed method can fully automate the extraction of an accurate set of 15 VCSEL parameters in real-time. In addition, is not limited to the proposed case but it is extensible to a larger number of parameters in more complex models.

References

[1] J. Diaci, D. Bračun, A. Gorkič, and J. Možina, "Rapid and flexible laser marking and engraving of tilted and curved surfaces," Opt Lasers Eng **49**, 195–199 (2011).

[2] J. Qi, K. Wang, and Y. Zhu, "A study on the laser marking process of stainless steel," J. Mater. Process. Technol. **139**, 273–276 (2003). IMCC2000 Vol. 2 S.I.

[3] M. Moradi, O. Mehrabi, T. Azdast, and K. Y. Benyounis, "Enhancement of low power CO2 laser cutting process for injection molded polycarbonate," Opt. Laser. Technol. **96**, 208–218 (2017).

[4] K. Salonitis, A. Stournaras, G. Tsoukantas, P. Stavropoulos, and G. Chryssolouris, "A theoretical and experimental investigation on limitations of pulsed laser drilling," J. Mater. Process. Technol. **183**, 96–103 (2007).

[5] G. Scotti, V. Matilainen, P. Kanninen, H. Piili, A. Salminen, T. Kallio, and S. Franssila, "Laser additive manufacturing of stainless steel micro fuel cells," J. Power Sources **272**, 356–361 (2014).

[6] E. Akman, A. Demir, T. Canel, and T. Sınmazçelik, "Laser welding of ti6al4v titanium alloys," J. Mater. Process. Technol. **209**, 3705–3713 (2009).

[7] Z. Ma and Y. Li, "Parameter extraction and inverse design of semiconductor lasers based on the deep learning and particle swarm optimization method," Opt. Express **28**, 21971–21981 (2020).

[8] https://www.synopsys.com/photonic-solutions/pic-design-suite.html.

[9] P. Mena, J. Morikuni, S.-M. Kang, A. Harton, and K. Wyatt, "A comprehensive circuit-level model of vertical-cavity surface-emitting lasers," J. Light. Technol. **17**, 2612–2632 (1999).

[10] M. X. Jungo, D. Erni, and W. Bachtold, "VISTAS: a comprehensive system-oriented spatiotemporal VCSEL model," IEEE J. Sel. Top. Quantum Electron. **9**, 939–948 (2003).

[11] P. Bardella, W. W. Chow, and I. Montrosset, "Design and analysis of enhanced modulation response in integrated coupled cavities DBR lasers using photon-photon resonance," Photonics **3** (2016).

[12] I. Khan, L. Tunesi, M. U. Masood, E. Ghillino, P. Bardella, A. Carena, and V. Curri, "A neural network-based automatized management of N× N integrated optical switches," in *Photonic Networks and Devices,* (OSA, 2021), pp. NeF2B–2.